6. Hoehn MM, Yahr MD. Parkinsonism: onset, progression, and mortality. *Neurology* 1967;17:21–25.
7. Fahn S, Elton RL, and the UPDRS Development Committee. Unified Parkinson disease rating scale. In: Fahn S, Marsden CD, Calne D, Goldstein M, eds. *Recent developments in Parkinson's disease*, vol. 2. Floral Park, New Jersey: Macmillan; 1987:293–304.
8. Robeson W, Dhawan V, Takikawa S, et al. SuperPETT 3000 time-of-flight tomograph: optimization of factors affecting quantification. *IEEE Trans Nucl Sci* 1993;40:135–142.
9. Hariz MI, Erikson AT. Reproducibility of repeated mounting of a noninvasive CT/MRI stereoadapter. *Appl Neurophysiol* 1986;49:336–347.
10. Luxen A, Milton P, Bida GT, et al. Remote, semiautomated production of 6-[^{18}F]fluoro-L-dopa for human studies with PET. *Appl Radiat Isot* 1990;41:275–281.
11. Melega WP, Grafton ST, Huang SC, Satyamurthy N, Phelps ME, Barrio JR. L-6-[^{18}F]fluoro-DOPA metabolism in monkeys and human: biochemical parameters for the formation of tracer kinetic models with PET. *J Cereb Blood Flow Metab* 1991;11:890–897.
12. Dhawan V, Jarden JO, Strother S, Rottenberg DA. Effect of blood curve smearing on the accuracy of parameter estimates obtained for ^{82}Rb/PET studies of blood-brain barrier permeability. *Phys Med Biol* 1988;33:61–74.
13. Eidelberg D, Takikawa S, Dhawan V, et al. Striatal ^{18}F-DOPA uptake: absence of an aging effect. *J Cereb Blood Flow Metab* 1993;13:881–888.
14. Chaly T, Bandyopadhyay D, Matacchieri R, Belakhlef A, Dhawan V, Takikawa S, Robeson W, Margouleff D, Eidelberg D. A disposable synthetic unit for the preparation of 3-O-Methyl-6-[^{18}F]fluorodopa using a regioselective fluorodemercuration reaction. *J Appl Radiat Isot* 1993;45:25–30.
15. Spetsieris P, Dhawan V, Takikawa S, Margouleff D, Eidelberg D. A versatile graphics-image processing package for imaging cerebral function. *IEEE Computer Graphics and Applications* 1993;13:15–26.
16. Talairach J, Tournoux P. *Co-planar stereotaxic atlas of the human brain*. New York: Thieme Medical Publishers, Inc., 1988.
17. Doudet DJ, McLellan CA, Carson R, et al. Distribution and kinetics of 3-O methyl-6-[^{18}F]fluoro-L-DOPA in the rhesus monkey brain. *J Cereb Blood Flow Metab* 1991;11:726–734.
18. Wahl LM, Chirakal R, Firnau, et al. The distribution and kinetics of [^{18}F]6-Fluoro-3-O methyl-L-dopa in the human brain. *J Cereb Blood Flow Metab* 1993;14:664–670.
19. Firnau G, Sood S, Chirakal R, Nahmias C, Garnett S. Cerebral metabolism of 6-[^{18}F]fluoro-L-3,4-Dihydroxyphenylalanine in the primate. *J Neurochem* 1987;29:1077–82.
20. Reith J, Dyve S, Kuwabara H, Guttman M, Diksic M, Gjedde A. Blood-brain transfer and metabolism of 6-[^{18}F]fluoro-L-Dopa in rat. *J Cereb Blood Flow Metab* 1990;10:707–719.

21. Akaike A. Posterior probabilities for choosing a regression model. *Ann Inst Math Sci* 1978;30:9–14.
22. Patlak CS, Dhawan V, Takikawa S, et al. Estimation of striatal uptake rate constant of FDOPA using PET: methodological issues. *Ann Nucl Med* 1993;7(suppl):S46–S47.
23. Hoshi H, Kuwabara H, Léger G, Cumming P, Guttman M, Gjedde A. 6-[^{18}F]fluoro-L-Dopa metabolism in living human brain: a comparison of six analytical methods. *J Cereb Blood Flow Metab* 1993;13:57–69.
24. Anderson TW. *An introduction to multivariate statistical analysis*. New York: John Wiley & Sons; 1984.
25. Takikawa S, Dhawan V, Chaly T, et al. Input functions for 6-[fluorine-18]fluorodopa quantitation in parkinsonism: comparative studies and clinical correlations. *J Nucl Med* 1994;35:955–963.
26. Firnau G, Sood S, Chirakal R, Nahmias C, Garnett S. Metabolites of 6-[^{18}F]fluoro-L-Dopa in human blood. *J Nucl Med* 1988;29:363–369.
27. Eidelberg D, Moeller JR, Dhawan V, et al. The metabolic anatomy of Parkinson's disease: complementary [^{18}F]fluorodeoxyglucose and [^{18}F]fluorodopa positron emission tomographic studies. *Mov Disorders* 1990;5:203–213.
28. Koeppe R, Mangner T, Betz AL, et al. Use of [^{11}C]aminocyclohexanecarboxylate for the measurement of amino acid uptake and distribution volume in human brain. *J Cereb Blood Flow Metab* 1990;10:727–739.
29. Cumming P, Kuwabara H, Gjedde A. A kinetic analysis of 6-[^{18}F]fluoro-L-Dihydroxyphenylalanine metabolism in the rat. *J Neurochem* 1994;63:1675–1682.
30. Ishikawa T, Dhawan V, Chaly T, et al. Clinical significance of striatal DOPA decarboxylase activity in Parkinson's disease. *J Nucl Med* 1996;37:216–222.
31. Carson RE, Doudet DJ, McLellan, et al. Combined modeling analysis of 6-[F-18]fluoro-L-dopa (FDOPA) and 3-O-methyl-6-[F-18]fluoro-l-dopa (OMFD) in nonhuman primates. *J Nucl Med* 1992;33:945.
32. Ishikawa T, Dhawan V, Chaly T, et al. [^{18}F]fluoro-L-dopa (FDOPA/PET) with an inhibitor of catechol-O-methyltransferase: effect of the plasma 3-O-methyldopa fraction on data analysis [Abstract]. *J Nucl Med* 1995;36(suppl):186P.
33. Laihinen A, Rinne JO, Rinne UK, et al. [^{18}F]-6-Fluorodopa PET scanning in Parkinson's disease after selective COMT inhibition with nitecapone (OR-462). *Neurol* 1992;42:199–203.
34. Gunther I, Psylla M, Antonini, et al. [^{18}F]Fluoro-L-dopa (FD) uptake and arterial plasma tracer metabolite alterations as a result of catechol-O-methyl transferase (COMT) and L-aromatic-amino-acid-decarboxylase (AAAD). *Neurology* 1993;43:A196.
35. Mannisto PT, Tuomainen P, Tuominen RK. Different in vivo properties of three new inhibitors of catechol O-methyltransferase in the rat. *Br J Pharmacol* 1992;105:569–574.

Clinical Significance of Striatal DOPA Decarboxylase Activity in Parkinson's Disease

Tatsuya Ishikawa, Vijay Dhawan, Thomas Chaly, Claude Margouleff, William Robeson, J. Robert Dahl, Francine Mandel, Phoebe Spetsieris and David Eidelberg

The Departments of Neurology, Research, Medicine and Biostatistics, North Shore University Hospital/Cornell University Medical College, Manhasset, New York

We performed dynamic PET studies with fluorodopa (FDOPA) in 9 normal volunteers and 16 patients with Parkinson's disease to investigate the applicability of dopa decarboxylase (DDC) activity measurements as useful markers of the parkinsonian disease process. **Methods:** From the 3-O-methyl-FDOPA (3OMFD)/PET studies, we obtained mean population values of the kinetic rate constants for 3OMFD ($K_1^M = 0.0400$ and $k_2^M = 0.0420$). We applied these values to calculate striatal DDC activity using the FDOPA compartmental model. We estimated k_3^D in this group using dynamic FDOPA-PET and population mean K_1^M and k_2^M values. We then applied the mean population K_1^M and k_2^M values to estimate k_3^D(pop) to a new group (6 normal volunteers and 11 patients) studied only with dynamic FDOPA-PET. In all FDOPA/PET studies, we calculated striatal uptake rate constants (K_i^{FD}) using a graphical method and also measured the striato-occipital ratio (SOR). **Results:** Although DDC activity has been postulated as a precise indicator of presynaptic nigrostriatal dopaminergic function, K_i^{FD} and SOR provided better between-group discrimination than did estimates of striatal DDC activity. K_i^{FD} and k_3^D(pop) both correlated significantly with quantitative disease severity ratings, with a similar degree of accuracy ($r = 0.69$ and 0.63 for k_3^D(pop) and K_i^{FD}, respectively; $p < 0.01$). **Conclusion:** Although estimated striatal DDC activity correlates with clinical disability, this measure is comparably less effective for early diagnosis. We conclude that a simple estimate such as striatal K_i^{FD} is superior to k_3^D measurements for most clinical and research applications.

Key Words: DOPA decarboxylase activity; PET; parkinsonism

J Nucl Med 1996; 37:216–222

Parkinson's disease is characterized by presynaptic nigrostriatal dopamine dysfunction. PET and 6-[^{18}F]fluoro-L-dopa (FDOPA) have been used to assess the presynaptic nigrostriatal dopaminergic function in life, to provide an objective measure of disease severity in Parkinson's disease patients and to
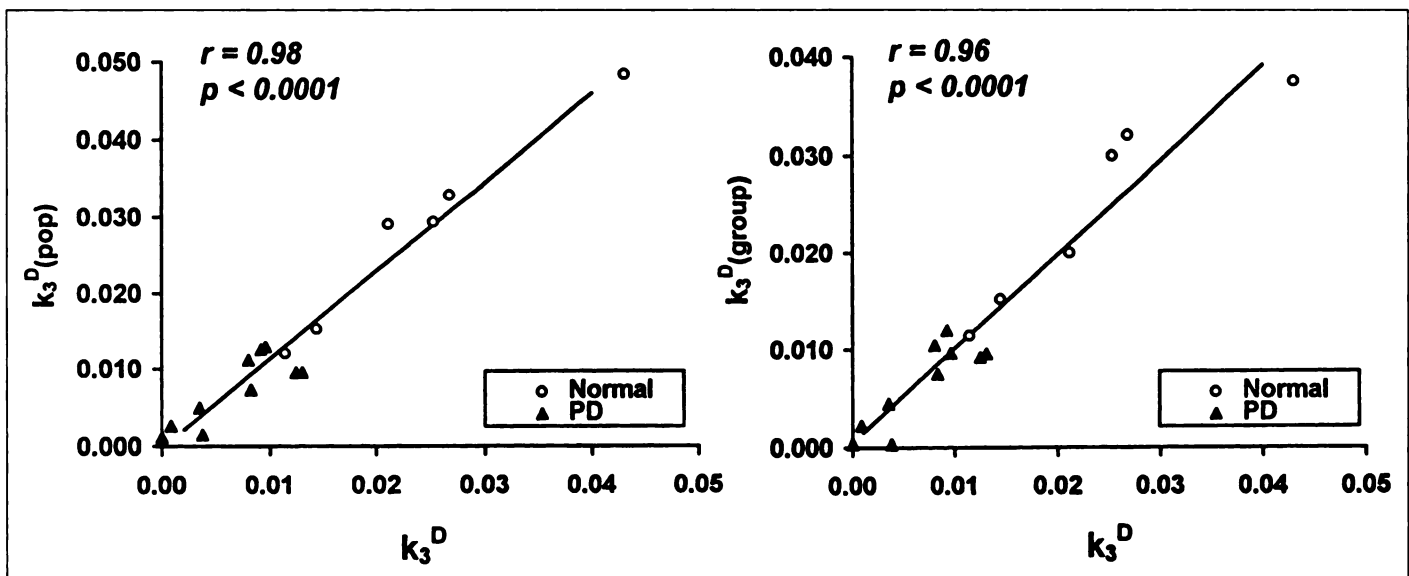
FIGURE 1. Correlations of striatal k_3^D measured with individual subject 3OMFD kinetic rate constants with: (A) k_3^D(pop) values estimated with mean total population values and (B) k_3^D(group) values estimated with mean group values (see text). Open circles (O) and closed triangles (▲) represent the left and right individual values for controls and Parkinson's disease patients, respectively. Individually derived k_3^D were highly correlated with k_3^D(pop) (r = 0.98, p = 0.0001; left panel) and with k_3^D(group) (r = 0.96, p = 0.0001; right panel).

identify individuals with early or preclinical involvement. The tracer is converted to 6-[^{18}F]fluorodopamine (FDA) by dopa decarboxylase (DDC) and retained in the striatum.

Various analytical methods have been developed to quantitate FDOPA/PET images. Simple target-to-background calculations from the striatum and occipital regions have provided useful information (1,2). Subsequently, the multiple time graphical approach (MTGA) (3) has been developed for the estimation of kinetic rate constants for striatal FDOPA uptake (K_i's) based upon the time courses of striatal and plasma FDOPA radioactivity (4,5). Alternatively, investigators have employed the plasma ^{18}F time-activity curve (TAC) without HPLC metabolite correction (6), and the occipital TAC without blood sampling (7,8). These uptake constants of FDOPA are not specific to the DDC activity in the striatum, because the uptake could be affected directly by changes in the transport system across the blood-brain barrier (BBB).

Compartmental analyses of FDOPA metabolism have been performed to calculate DDC activity (k_3^D), as a more sensitive measure of nigrostriatal dopaminergic function (9). Most of these approaches account for the biodistribution of 3-O-methyl-FDOPA (3OMFD), the major metabolite of FDOPA which crosses the BBB without trapping. Previously, 3OMFD distribution parameters have been assumed either based on rat data (10,11) or modeling constraints (12). We calculated kinetic parameters for FDOPA based on the combined FDOPA and 3OMFD/PET studies in eight subjects, and found that the variability of K_1^M and k_2^M values was small (13). These measures are similar to the values reported in rhesus monkeys (14) and in humans (15). We therefore validated the use of the population mean values for K_1^M and k_2^M to estimate striatal DDC activity from dynamic FDOPA/PET without requiring individual measurements of these parameters with adjunctive 3OMFD/PET. We studied 16 mild-to-severely affected Parkinson's disease patients and 9 normal control subjects with FDOPA/PET and examined the clinical correlates of the estimated measures of striatal DDC activity. We compared the diagnostic power of these estimated k_3^D values with simpler measures, such as graphically derived FDOPA uptake rate constants (K_i^{FD}) and striato-occipital ratios (SORs).

MATERIALS AND METHODS

Subjects

Group A. This group consisted of the five Parkinson's disease patients and three normal volunteers studied with both FDOPA and 3OMFD/PET, reported by us in the accompanying paper (13). We explored the possibility of using the mean values for striatal K_1^M and k_2^M values determined across the total population of normal and Parkinson's disease patients (0.0400 and 0.0420, respectively) (13) in the calculation of striatal k_3^D from the FDOPA scans alone. These estimated values were designated k_3^D(pop). Additionally, because of the possibility of small differences in K_1^M and k_2^M between normal controls and Parkinson's disease patients, we also calculated estimates derived using separate mean values for the two subject groups. These values were designated k_3^D(group). We computed striatal k_3^D(pop) and k_3^D(group) values using the model described by us (13), setting k_5^D, k_7^D and k_9^D all to 0 min^{-1}, where k_5^D is the O-methylation coefficient of FDOPA, k_7^D is the lumped O-methylation and oxidation coefficient of FDA (fluorodopamine), and k_9^D is the fractional clearance from brain of the diffusible FDA metabolites (13).

These estimates were correlated with the previously published striatal k_3^D values calculated in each subject using individually measured K_1^M and k_2^M values from 3OMFD/PET. We noted a close relationship between actual striatal k_3^D (i.e., calculated using individually derived K_1^M and k_2^M values obtained from adjunctive 3OMFD/PET studies) and the estimated values (i.e., those calculated without individual 3OMFD/PET using whole population or subgroup mean values K_1^M and k_2^M values). We found that k_3^D correlated significantly with both k_3^D(pop) and k_3^D(group) estimates (r = 0.98 and 0.96 respectively, p < 0.0001; see Fig. 1). We therefore used total population mean K_1^M and k_2^M values as substitutes for the individually measured 3OMFD rate constants in the calculation of striatal k_3^D in this and the subsequent subject group.

Group B. We studied a second entirely different population of Parkinson's disease patients and normal subjects with FDOPA/PET and used the population values of mean K_1^M and k_2^M determined above (Group A) to calculate striatal k_3^D(pop) on an individual basis. This group consisted of the six normal volunteer

TABLE 1
Group B Parkinson's Disease Patients*

Patient no.	Age (yr)	Sex	H&Y	Tremor	Rigidity	Gait	A.I.	UPDRS
1	50	M	I	0	0	0	−1	1
2	71	M	I	1	2	0	3	8
3	54	M	I	2	1	0	6	7
4	50	M	I	0	2	0	5	5
5	38	M	II	4	0	0	4	12
6	46	M	III	0	5	1	2	14
7	67	M	III	0	4	2	−2	19
8	69	F	III	3	5	2	1	24
9	84	M	III	10	4	2	−5	33
10	58	F	IV	2	7	4	2	32
11	54	M	V	1	13	4	−1	47

*See Table 1 in accompanying paper for Group A patients (13).

H&Y = Hoehn and Yahr Stage; AI = asymmetry index calculated by subtracting the left UPDRS scores from the right scores. Positive AI reflects a higher clinical involvement of the right body side; UPDRS = Unified Parkinson Disease Rating Scale composite scores [UPDRS 3.0; items 19–31, (22)].

TABLE 2
Striatal Dopa Decarboxylase Activity $(k_3{}^D)$, $K_i{}^{FD}$ and Striatal-to-occipital Ratio

		$k_3{}^D$(pop)*	$k_3{}^D$(M2)*	$k_3{}^D$(M3)*	$K_i{}^{FD}$*	SOR
Normal (n = 9)	Mean	0.0206	0.0820	0.0065	0.0143	2.19
	s.d.	0.0097	0.0507	0.0031	0.0028	0.23
	COV	47%	62%	48%	19%	11%
PD (n = 16)	Mean	0.0099	0.0336	0.0046	0.0074	1.60
	s.d.	0.0074	0.0174	0.0033	0.0028	0.18
	COV	74%	52%	71%	37%	11%

*$k_3{}^D$(pop), $k_3{}^D$(M2) and $k_3{}^D$(M3) are expressed as min^{-1} and $K_i{}^{FD}$ as ml/min/gm.

PD = Parkinson's Disease; COV = coefficient of variation defined as (s.d./mean) × 100 (%); SOR = striatal-to-occipital ratio.

subjects (3 men and 3 women; mean age ± s.d., 51 ± 19 yr; range 19–71 yr) and 11 classical Parkinson's disease patients without dementia (8 men and 3 women; age 58 ± 13 yr). This group was selected with mild to severe clinical involvement [Hoehn and Yahr Stages I–V (16); see Table 1].

PET and Image Analysis

Details regarding PET and region of interest (ROI) analysis are given in an accompanying paper (13).

In each member of Groups A and B, kinetic measures for striatal FDOPA uptake were graphically calculated by the multiple time graphical approach (MTGA) (3) using the time course of striatal radioactivity, and the input function for plasma FDOPA determined using plasma arterial blood sampling and HPLC analysis (17). The time course of specific (background subtracted) striatal concentration divided by plasma FDOPA activity was plotted against the ratio of the plasma time-integral to the plasma FDOPA concentration. In the MTGA, the slope of the this line represents the rate constant of FDOPA uptake into the striatum $(K_i{}^{FD})$ (3–7). We also calculated the striatal-to-occipital activity ratio (SOR) by dividing striatal count rates by the occipital count rate measured on the last 10-min scan (90–100 min postinjection).

In addition to these standard FDOPA/PET measurements, we estimated striatal DDC activity $(k_3{}^D)$ using three modeling approaches: (1) The compartmental model in which we used the mean population values of striatal $K_1{}^M$ and $k_2{}^M$ (0.0400 and 0.0420, respectively) in the analysis of the kinetic FDOPA/PET data to calculate striatal $k_3{}^D$(pop) (see above). We set the values of striatal $k_5{}^D$, $k_7{}^D$, and $k_9{}^D$ all to 0 min^{-1}, and estimated striatal $K_1{}^D$, $k_2{}^D$, $k_3{}^D$(pop), and V_b, the brain vascular volume. (2) The compartment analysis proposed by Kuwabara et al. (11) which assumes the common partition volume $(V_e = K_1/k_2)$ for the frontal lobe and striatum, and fixes the K_1 ratio between FDOPA and OMFD (q = 2.3), where K_1 and k_2 are the unidirectional blood-brain clearances for FDOPA and 3OMFD (with superscripts D and M, respectively). The values of striatal $k_5{}^D$, $k_7{}^D$, $k_9{}^D$ were set to 0, 0.02, and 0.005 min^{-1}. We have designated values of $k_3{}^D$ estimated in this manner as $k_3{}^D$(M2) (13). We also used this model to estimate striatal $K_1{}^D$ and V_b, the brain vascular volume. (3) The two-compartment, three-parameter model in which the presence of 3OMFD is completely neglected and total plasma ^{18}F activity is used as an input function (18). We estimated striatal $K_1{}^D$, $k_2{}^D$ and $k_3{}^D$(M3). These calculations were performed using software

designed for the statistical analysis of nonlinear models (PCNONLIN, SCI software; Lexington, KY).

Statistical Analysis

The following statistical procedures were performed using SAS (SAS Institute; Cary, NC): (1) The accuracy of between-group discrimination of Parkinson's disease patients and normals was assessed for each of the parameters [$K_i{}^{FD}$, SOR, $k_3{}^D$(pop), $k_3{}^D$(M2), $k_3{}^D$(M3)] using a stepwise procedure with the F-test associated with Wilk's lambda (19). In this analysis, mean left and right striatal measures for the Parkinson's disease patients were compared with mean striatal values measured for the normal volunteers. (2) We correlated mean striatal $k_3{}^D$(pop), $k_3{}^D$(M2), $k_3{}^D$(M3), $K_i{}^{FD}$ and SOR values with UPDRS composite motor scores [UPDRS 3.0; items 19–31; (20)] for the Parkinson's disease patients in Groups A and B by computing Pearson Product-Moment Correlation Coefficients. In addition, we compared differences between these clinical correlations using Student's t-tests. (3) We correlated age with $k_3{}^D$(pop), $k_3{}^D$(M2) and $k_3{}^D$(M3) in the normal subjects in Groups A and B by computing Pearson product-moment correlation coefficients.

RESULTS

Mean values, standard deviations and coefficients of variation (COVs) of striatal $k_3{}^D$(pop), $k_3{}^D$(M2), $k_3{}^D$(M3), $k_i{}^{FD}$ and SOR are given in Table 2. In the combined Group A and B (A + B), discriminant analysis indicated that $K_i{}^{FD}$ and SOR distinguished Parkinson's disease patients from normals more accurately than DDC activities, although $k_3{}^D$(M2) and $k_3{}^D$(pop) discriminants were also highly significant (F[1, 23] = 37.3, 54.2, 12.3, and 10.2; p = 0.0001, 0.0001, 0.002, and 0.004 for $K_i{}^{FD}$, SOR, $k_3{}^D$(M2) and $k_3{}^D$(pop), respectively; see Fig. 2). On the other hand, $k_3{}^D$(M3) failed to discriminate between groups (F[1, 23] = 3.046, p = 0.09). In Group B alone, all between group discriminations were significant except those obtained with $k_3{}^D$(M2), $k_3{}^D$(pop), and $k_3{}^D$(M3) (F[1, 15] = 18.0, 23.3, 4.2, 2.5, and 0.003; p = 0.0007, 0.0002, 0.058, 0.133 and 0.954 for $K_i{}^{FD}$, SOR, $k_3{}^D$(M2), $k_3{}^D$(pop) and $k_3{}^D$(M3), respectively).

In the Parkinson's disease group, correlation analysis revealed a significant negative relationship between UPDRS composite scores and striatal $K_i{}^{FD}$ (r = −0.69, p < 0.03 for Group B; r = −0.62, p < 0.01 for the combined Group A + B); $k_3{}^D$(pop) (r = −0.77, p < 0.006 for Group B; r = −0.66, p < 0.006 for Group A + B) and $k_3{}^D$(M2) (r = −0.75, p < 0.008 for Group B; r = −0.63, p < 0.009 for Group A + B). These clinical scores did not correlate significantly with $k_3{}^D$(M3) (r = 0.60, p = 0.06 for Group B; r = 0.48, p = 0.06 for Group A + B) and SOR values (r = 0.40, p = 0.23 for Group B; r = 0.37, p = 0.17 for Group A + B) (Fig. 3). The correlation coeffi-

FIGURE 2. Discriminant analyses between Parkinson's disease patients and normal subjects for k_3^D(pop), k_3^D(M2), k_3^D(M3), K_i^{FD} and SOR (see text). K_i^{FD} and SOR separated Parkinson's disease patients from normals more accurately than estimates of striatal DDC activity, although these measures were also highly significant except for k_3^D(M3) (F[1, 23] = 37.3, 54.2, 12.3, 10.2 and 3.0; p = 0.0001, 0.0001, 0.002, 0.004 and 0.09 for K_i^{FD}, SOR, k_3^D(M2) k_3^D(pop), and k_3^D(M3), respectively).
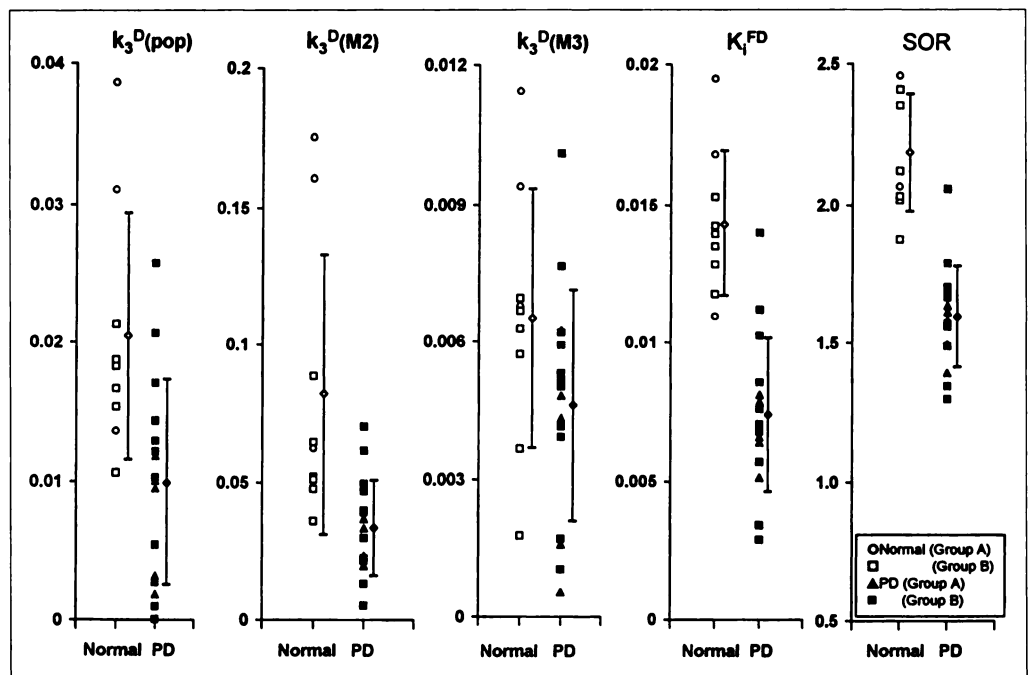
cients were not found to be statistically different in Group B as compared with the combined Group A + B (Group A was considered too small for independent comparison).

In the nine normal subjects included in combined Group A + B (range 19–71 yr), neither striatal DDC activity (k_3^D) nor K_i^{FD} correlated significantly with chronological age [k_3^D(pop): r = 0.31, p = 0.42 (Fig. 4, left panel); k_3^D(M2): r = 0.54, p = 0.15; k_3^D(M3): r = 0.46, p = 0.22; K_i^{FD}: r = 0.21, p = 0.58 (Fig. 4, right panel).

DISCUSSION

Population 3OMFD Kinetic Rate Constants: Application for Kinetic FDOPA-PET to Estimate Striatal DDC Activity

FDOPA is metabolized rapidly in the plasma by COMT to 3OMFD, especially following pretreatment with carbidopa (21). Both FDOPA and 3OMFD cross the blood-brain barrier

using the large neutral amino acid (LNAA) transporter (22). Thus, the presence of plasma 3OMFD activity in the kinetic analysis of FDOPA/PET data can affect the estimation of striatal DDC activity (k_3^D) (13). Compartmental modeling approaches of FDOPA kinetics, taking into account the contribution of 3OMFD, have been proposed by Kuwabara et al. (11) and Huang et al. (12) using a single reversible compartment to model the kinetics of OMFD in the brain. Huang et al. (12) fixed K_1^M to be 1.7 times greater than K_1^D based on a residual sum of squares, while Kuwabara et al. (11) fixed their K_1^M/K_1^D at 2.3, based upon experimental rat data (10). These assumed ratios yield over estimates of striatal K_1^M (0.0759 and 0.0532 for the Kuwabara (11) and Huang (12) models, respectively) as compared to values obtained empirically with 3OMFD/PET. Indeed, independent measurements in the rhesus monkey (14) yielded striatal K_1^M and k_2^M to be 0.043 and 0.043, respec-

FIGURE 3. Correlations of mean striatal k_3^D(pop), k_3^D(M2), K_i^{FD} and SOR values with UPDRS composite motor scores (see text). Significant negative correlations between the clinical motor ratings and the FDOPA-PET parameters were observed: (A) Striatal K_i^{FD}: r = −0.62, p < 0.01 (lower left panel); (B) Striatal k_3^D(M2): r = −0.63, p < 0.009 (upper right panel); (C) Striatal k_3^D(pop): r = −0.66, p < 0.006 (upper left panel). (D) Clinical scores did not correlate with SOR values (lower right panel).
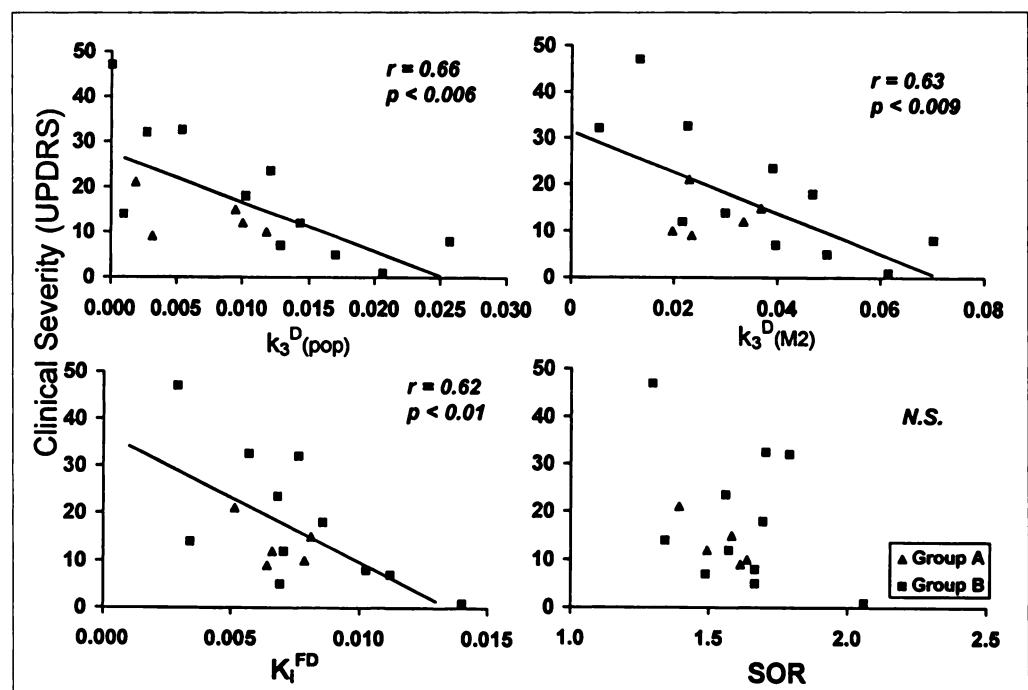
FIGURE 4. Correlation of striatal $k_3{}^D$(pop) and $K_i{}^{FD}$ with age in nine normal subjects (range 19–71 yr). Open circles (O) denote Group A normals; open squares (□) denote Group B normals. Significant aging correlations were not observed with estimated striatal DDC activity ($k_3{}^D$(pop): r = 0.31, p = 0.42; left panel) or with striatal $K_i{}^{FD}$ (r = 0.21, p = 0.58; right panel).
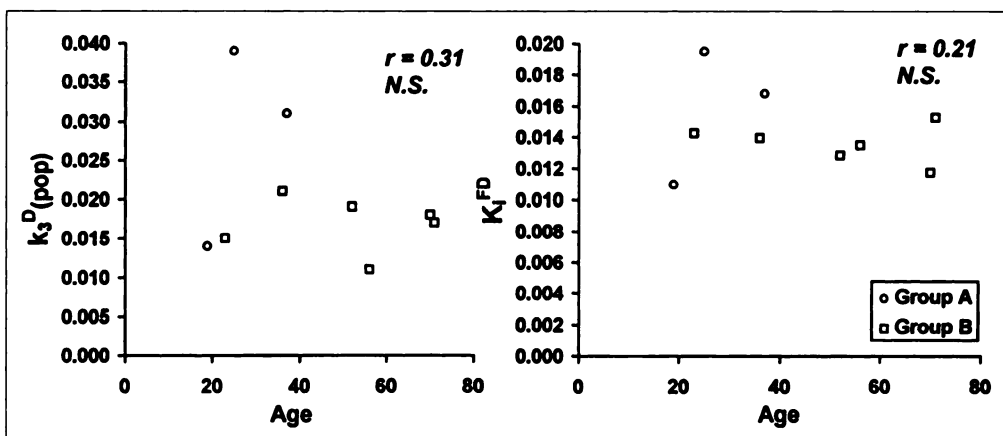
tively, consistent with the analogous measures obtained in human 3OMFD/PET studies (13,15). Moreover, these independent estimates are in good agreement with transport rate constants for the synthetic amino acid [^{11}C]aminocyclohexanecarboxylate, which enters the brain utilizing the same transport system as 3OMFD (23). This assumption-driven overestimation of $K_1{}^M$ can produce an error in the subsequent estimates of $k_3{}^D$ (13). For example, $k_3{}^D$ obtained by the method proposed by Kuwabara et al. (11) resulted in a value 2–4 times higher than that estimated with individual $K_1{}^M$ and $k_2{}^M$ values. In another modeling approach (18), in which the contribution of 3OMFD is completely ignored, $k_3{}^D$ values were estimated to be 2–4 times lower. Thus, selection of appropriate $K_1{}^M$ and $k_2{}^M$ values may be critical to all models used to obtain accurate $k_3{}^D$ estimates in kinetic FDOPA/PET studies.

Ideally, individual kinetic rate constants for 3OMFD should be obtained independently in each subject to estimate striatal $k_3{}^D$ accurately. This, however, requires independent dynamic 3OMFD/PET studies with subsequent FDOPA/PET, both of which involve extensive blood sampling and HPLC. In our study, we found the coefficient of variation for $K_1{}^M$ and $k_2{}^M$ to be 36% and 30%, respectively, suggesting the possibility of a mean population approach in fixing these parameters. Indeed, we found that the use of population mean rate constants for 3OMFD transport provides an acceptable alternative to adjunctive 3OMFD/PET studies in the calculation of striatal $k_3{}^D$. Striatal DDC activity calculated with population $K_1{}^M$ and $k_2{}^M$ values [$k_3{}^D$(pop)] was highly correlated with $k_3{}^D$ calculated with individually determined $K_1{}^M$ and $k_2{}^M$ values ($R^2 > 0.98$, $p < 0.0001$). Although a difference in OMFD kinetic rate constants may exist between Parkinson's disease patients and normals (13), estimates performed using the subgroup mean values [$k_3{}^D$(group)] did not provide better correlations with actual $k_3{}^D$ than the mean 3OMFD values for the whole population. Thus, in lieu of individually derived rate constants we used total population mean 3OMFD values in the FDOPA model to estimate $k_3{}^D$. We then used estimated $k_3{}^D$(pop) values to assess the clinical significance of striatal DDC activity measurements. Additionally, as there was no significant difference in the clinical-PET correlations obtained in Group B patients and those from Groups A and B combined (Group A alone was too small for independent statistical analysis), we assessed the clinical significance of estimated DDC activity ($k_3{}^D$(pop), $k_3{}^D$(M2) or $k_3{}^D$(M3)) across the entire population comprising Groups A and B together.

Early Diagnosis

We have recently reported that Ki^{FD} may be the optimum FDOPA-PET marker for the parkinsonian disease process

because of its comparative superiority in discriminating mildly affected normals and in predicting clinical severity of disease (24). We also noted that a simple semiquantitative index, SOR, is nearly as sensitive an early disease discriminator as striatal $K_i{}^{FD}$, suggesting that kinetic measures may not necessarily be needed for early disease detection. In this study, we note that although DDC activity measures ($k_3{}^D$(pop) or $k_3{}^D$(M2)) can discriminate Parkinson's disease patients from normals, these parameters were not as accurate for this purpose as SOR and $K_i{}^{FD}$. One reason for the comparative weakness of striatal DDC activity is its inherent noise (COV ~ 45% in normals), making its discriminant accuracy less than that of SOR and $K_i{}^{FD}$ (13) (also see Table 2). Our findings contrast with those of Hoshi et al. (25) who reported that measures of striatal DDC activity ($k_3{}^D$(M2)) could better differentiate Parkinson's disease patients from normal controls than $K_i{}^{FD}$. This disparity may be due to differences in patient selection. The clinical severity of the Parkinson's disease patients differed markedly between their study and ours. Whereas all six patients studied by those investigators were all moderately to severely affected patients [H&Y Stage III or IV], our 16 subjects included a clinically wide range of patients, from mild to severe [H&Y Stage I to V]. Indeed, had we selected only moderately to severely affected patients, striatal DDC activity ($k_3{}^D$(M2) or $k_3{}^D$(pop)) would discriminate the two groups. On the other hand, FDOPA/PET measures of striatal DDC activity can not discriminate early Parkinson's disease patients from normals (see below). Another estimate of striatal DDC activity, $k_3{}^D$(M3), neither discriminated Parkinson's disease patients from normals nor significantly correlated with UPDRS ratings. Thus, the simplified and mathematically justifiable model (18) failed to provide us with accurate and clinically valuable measures as compared to other analytical methods. This suggests the importance of proper accounting for the presence of 3OMFD fraction in the compartmental modeling approach.

Disease Severity Assessment

Quantitative clinical severity measures correlated significantly with striatal DDC activity and $K_i{}^{FD}$, but not with SOR. Indeed, all three parameters which correlated significantly with UPDRS ratings, $k_3{}^D$(pop), $k_3{}^D$(M2) and $K_i{}^{FD}$ yielded predictions of clinical severity of similar accuracy ($R^2 \sim 0.40$). Interestingly, SOR failed to correlate significantly with UPDRS despite being the most accurate discriminator between Parkinson's disease patients and normals in the same group of the patients. When we estimated SOR from the fitted striatal and occipital count from the dynamic dataset, however, SOR measures significantly correlated with UPDRS (r = 0.59, p < 0.02). This disparity probably occurs because the simple SOR,

calculated from the last 10-min scan, can contain errors from low count rates with striatum and occipital cortex. In Parkinson's disease patients in particular, where the striatal counts are significantly reduced, SOR correlation with UPDRS ratings may be masked by this type of measurement error. By contrast, even though k_3^D(M2) are based on high estimates of the 3OMFD transport rate constants (13), these parameters still correlated with clinical severity ratings well.

The loss of nigrostriatal dopaminergic projections can be compensated for to some extent by an upregulation of DDC activity. As a result, DDC activity per unit volume may remain close to normal, especially in the early stages of parkinsonism. Indeed, the early stages of disease are associated with approximately 60% nigral nerve cell loss (26). This suggests that the maximal upregulation of DDC activity is not capable of compensating the dopaminergic cell loss beyond this degree. We speculate that once striatal DDC activity has been maximally upregulated, it may then accurately represent the residual number of intact dopaminergic terminals. Thus, striatal DDC activity as measured with FDOPA-PET may be considered to represent the compensatory reserve of the presynaptic nigrostriatal dopamine system in preclinical stages of the illness. With established disease, these measures may be more representative of actual numbers of nigral neurons (27) and, therefore, correspond linearly with overall clinical disease progression.

In this vein, we found that striatal k_3^D reductions did not correlate with chronological age in normals. The issue of striatal FDOPA uptake in normal aging is still controversial (28). Striatal FDOPA influx rate constants have been reported to correlate negatively with age in some studies ($29,30$) but not in others ($8,17$). The reasons for these differences have been discussed elsewhere (28). In conformity with the negative studies, estimation of striatal k_3^D(M2) by Murase et al. (31) in 26 normals failed to reveal a significant decline in this parameter with senescence. In our nine normal subjects, we also did not find a significant correlation between age and striatal DDC activity, estimated either as k_3^D(pop), k_3^D(M2) or k_3^D(M3). These studies suggest that the loss of the dopaminergic nigrostriatal terminals in aging may be compensated in part by upregulation of neuronal DDC activity. These findings are supported by the postmortem neurochemical study of Kish et al. (32), in which striatal DDC concentration did not decline appreciably with age.

Although k_3^D correlated with disease severity as accurately as K_i^{FD}, this measure has comparatively lower capacity for the discrimination of early affected patients. Additionally, even with the use of population kinetic rate constants for 3OMFD, the estimation of k_3^D(pop) still requires full dynamic FDOPA-PET imaging, as well as extensive arterial blood sampling and HPLC. On the other hand, we recently reported that K_i^{FD} can be accurately estimated ($R^2 > 0.98$) with a simplified population-derived FDOPA input function, requiring only two arterial blood samples and no HPLC (24). Given the technical demands of estimating k_3^D and the comparative advantage of K_i^{FD} for between-group discrimination and correlation with disease progression, we conclude that this measure is preferable to k_3^D for most clinical research applications. Moreover, with new high sensitivity tomographs, the straightforward measurement of SOR may prove to be a compatible alternative to the various kinetic parameters currently in use.

CONCLUSION

The mean population kinetic rate constants for 3OMFD can be applied in dynamic FDOPA-PET to estimate DDC activity [k_3^D(pop)]. Estimates of striatal DDC activity (k_3^D(pop), k_3^D(M2),

or k_3^D(M3)) cannot discriminate between normals and Parkinson's disease patients as accurately as K_i^{FD} or SOR. These estimates can, however, predict clinical severity but with accuracy that is not superior to the more simply obtained K_i^{FD} measure. Given its simplicity and convenience, the graphically derived striatal FDOPA uptake rate constant, K_i^{FD}, or its noninvasively derived analogues ($7,24$), proves to be optimal for the neuroimaging assessment of parkinsonism with FDOPA-PET.

REFERENCES

1. Garnett E, Nahmias C, Firnau G. Central dopaminergic pathways in hemiparkinsonism examined by positron emission tomography. *Can J Neurol Sci* 1984;11:174–179.
2. Leenders KL, Palmer AJ, Quinn N, et al. Brain dopamine metabolism in patients with Parkinson's disease measured with positron emission tomography. *J Neurol Neurosurg Psychiatry* 1986;49:853–860.
3. Patlak CS, Blasberg RG, Fenstermacher JD. Graphical evaluation of blood-to-brain transfer constants from multiple-time uptake data. *J Cereb Blood Flow Metab* 1983;3:1–7.
4. Martin WRW, Palmer MR, Patlak CS, Calne DB. Nigrostriatal function in humans studied with positron emission tomography. *Ann Neurol* 1989;26:535–542.
5. Eidelberg D, Moeller JR, Dhawan V, et al. The metabolic anatomy of Parkinson's Disease: complementary ^{18}F-fluorodeoxyglucose and ^{18}F-fluorodopa positron emission tomography studies. *Movement Disorders* 1990;5:203–351.
6. Leenders KL, Salmon EP, Tyrrell P, et al. The nigrostriatal dopaminergic system assessed in vivo by positron emission tomography in healthy volunteer subjects and patients with Parkinson's disease. *Arch Neurol* 1990;47:1290–1298.
7. Brooks DJ, Ibanez V, Sawle GV, et al. Differing patterns of striatal ^{18}F-Dopa uptake in Parkinson's disease, multiple system atrophy, and progressive supranuclear palsy. *Ann Neurol* 1990;28:547–555.
8. Sawle GV, Colebatch JG, Shah A, Brooks DJ, Marsden CD, Frackowiak SJ. Striatal function in normal aging: implications for Parkinson's disease. *Ann Neurol* 1990;28:799–804.
9. Gjedde A, Reith J, Dyve S, et al. Dopa decarboxylase activity of the living human brain. *Proc Natl Acad Sci* 1991;88:2721–1725.
10. Reith J, Dyve S, Kuwabara H, et al. Blood-brain transfer and metabolism of 6-[^{18}F]fluoro-L-dopa in rat. *J Cereb Blood Flow Metab* 1990;10:707–719.
11. Kuwabara H, Cumming P, Reith J, et al. Human striatal L-DOPA decarboxylase activity estimated in vivo using 6-[^{18}F]fluoro-DOPA and positron emission tomography: error analysis and application to normal subjects. *J Cereb Blood Flow Metab* 1993;13:43–56.
12. Huang SC, Yu DC, Barrio JR, et al. Kinetics and modeling of L-6-[^{18}F]Fluoro-DOPA in human positron emission tomographic study. *J Cereb Blood Flow Metab* 1991;11:898–913.
13. Dhawan V, Ishikawa T, Patlak C, et al. Combined FDOPA and 3OMFD PET studies in Parkinson's disease. *J Nucl Med* 1996;37:209–216.
14. Doudet DJ, McLellan CA, Carson R, et al. Distribution and kinetics of 3-O methyl-6-[^{18}F]fluoro-L-DOPA in the rhesus monkey brain. *J Cereb Blood Flow Metab* 1991;11:726–734.
15. Wahl L, Chirakal R, Firnau G, et al. The distribution and kinetics of [^{18}F]6-fluoro-3-O-methyl-L-dopa in the human brain. *J Cereb Blood Flow Metab* 1994;14:664–670.
16. Hoehn MM, Yahr MD. Parkinsonism: onset, progression and mortality. *Neurology* 1967;17:21–25.
17. Eidelberg D, Takikawa S, Dhawan V, et al. Striatal ^{18}F-DOPA uptake: absence of an aging effect. *J Cereb Blood Flow Metab* 1993;13:881–888.
18. Wahl LM, Garnett ES, Chirakai R, et al. Quantification of dopamine metabolism in man: what is the most justifiable approach? *J Cereb Blood Flow Metab* 1993;13:(suppl 1)S722.
19. Anderson TW. *An Introduction to Multivariate Statistical Analysis.* New York: John Wiley & Sons, 1984.
20. Fahn S, Elton RL, the UPDRS Development Committee. Unified Parkinson disease rating scale. In: Fahn S, Marsden CD, Calne D, Goldstein M, eds. *Recent developments in Parkinson's disease,* vol. 2. Floral Park, NJ: Macmillan; 1987:293–304.
21. Melega WP, Luxen A, Perlmutter MM, Nissenson CHK, Phelps ME, Barrio JR. Comparative in vivo metabolism of 6-[^{18}F]fluoro-L-DOPA and [^{3}H]L-DOPA in rats. *Biochem Pharmacol* 1990;39:1853–1860.
22. Oldendorf WH, Szabo J. Amino acid assignment to one of three blood-brain barrier amino acid carriers. *Am J Physiol* 1976;230:94–98.
23. Koeppe RA, Mangner T, Betz AL, et al. Use of [^{11}C]Aminocyclohexane-carboxylate for the measurement of amino acid uptake and distribution volume in human brain. *J Cereb Blood Flow Metab* 1990;10:727–739.
24. Takikawa S, Dhawan V, Chaly T, et al. Input functions for 6-[fluorine-18]fluorodopa quantitation in parkinsonism: comparative studies and clinical correlations. *J Nucl Med* 1994;35:955–963.
25. Hoshi H, Kuwabara H, Léger G, Cumming P, Guttman M, Gjedde A. 6-[^{18}F]fluoro-L-Dopa metabolism in living human brain: a comparison of six analytical methods. *J Cereb Blood Flow Metab* 1993;13:57–69.
26. Bernheimer H, Birkmayer W, Hornykiewicz O, et al. Brain dopamine and the syndromes of Parkinson and Huntington. *J Neurol Sci* 1973;20:415–455.

27. Snow BJ, Tooyama I, McGeer EG, et al. Human positron emission tomographic [¹⁸F]fluorodopa studies correlate with dopamine cell counts and levels. *Ann Neurol* 1993;34:324–330.
28. Letters to the editor. An aging effect in striatal fluorodopa uptake? Large versus small ROIs. *J Cereb Blood Flow Metab* 1994;14:882–883.
29. Martin WRW, Palmer MR, Patlak CS, et al. Nigrostriatal function in man studied with positron emission tomography. *Ann Neurol* 1989;26:535–542.
30. Vingerhoets FJG, Snow BJ, Sculzer M, et al. Reproducibility of fluorine-18-6-fluorodopa positron emission tomography in normal human subjects. *J Nucl Med* 1994;35:18–23.
31. Murase K, Kuwabara H, Cumming P, et al. Relative activity of dopa decarboxylase remained unchanged with age. *J Nucl Med* 1994;5(suppl):10P.
32. Kish SJ, Zhong XH, Hornykiewcz O, Haycock JW. Striatal 3,4,dihydroxyphenylalanine decarboxylase in aging: disparity between postmortem and positron emission tomography studies? *Ann Neurol* 1995;38:260–264.

Reproducibility of Iodine-123-β-CIT SPECT Brain Measurement of Dopamine Transporters

John P. Seibyl, Marc Laruelle, Christopher H. van Dyck, Elizabeth Wallace, Ronald M. Baldwin, Sami Zoghbi, Yolanda Zea-Ponce, John L. Neumeyer, Dennis S. Charney, Paul B. Hoffer and Robert B. Innis

Departments of Diagnostic Radiology and Psychiatry, Yale University School of Medicine, New Haven, Connecticut; Department of Veterans Affairs Medical Center, West Haven, Connecticut; and Research Biochemicals International, Natick, Massachusetts

Iodine-123-β-CIT has been used as a probe of monoamine transporters in human and nonhuman primates utilizing SPECT. To assess the utility of this tracer for measurement of striatal dopamine (DA) transporters in human disease, we studied the test/retest variability and reliability of SPECT measures obtained after bolus injection of [¹²³I]β-CIT 0–7 hr (Day 1) and 18–24 hr (Day 2) after administration. **Methods:** For the Day 2 study, seven healthy humans (4 men, 3 women; aged 19–74 yr) participated in two [¹²³I]β-CIT SPECT scans separated by 7–14 days. Subjects were imaged at 18, 21 and 24 hr postinjection of 370 MBq (10 mCi) [¹²³I]β-CIT. Two outcome measures were evaluated: (a) the ratio of specific striatal (activity associated with DA transporter binding) to nondisplaceable uptake, also designated V_3'' and (b) the total specific striatal uptake (%SSU) expressed as a percentage of injected radiotracer dose. Test/retest variability associated with V_3'' and total specific striatal uptakes were compared for scans acquired at 18, 21 and 24 hr with 24 hr only postinjection scans. For the Day 1 study, three of the subjects participated in two kinetic studies of [¹²³I]β-CIT uptake. A three-compartment model was used for determination of konBmax and binding potential (BP = B_{max}/K_d) and the reproducibility of the measures assessed. **Results:** In the Day 2 study, both outcome measures demonstrated excellent test/retest reproducibility with variability of $V_3'' = 6.8 \pm 6.8\%$ and percent striatal uptake = 6.6 ± 4.3% using data acquired from all time points. There were no significant differences in variability for the two outcome measures obtained. The intraclass correlation coefficient ρ was 0.96 and 0.98 for V_3'' and %SSU, respectively. Considering the 24 hr postinjection scans only, there was a nonsignificant trend toward lower test/retest variability for %SSU compared to V_3'' (6.6 ± 4.2% and 12.8 ± 9.0%, respectively). The test/retest variability for the Day 1 kinetic modeling data showed marked differences depending on the fitting strategy and assumptions about the reversibility of [¹²³I]β-CIT in striatum. Using a model that assumed a low, fixed value for reversible striatal binding (k_4) produced low variability (12 ± 9%). **Conclusion:** These data suggest that SPECT imaging performed at either 0–7 hr or 18–24 hr after [¹²³I]β-CIT injection permits calculation of reliable and reproducible measures of dopamine transporters and supports the feasibility of using [¹²³I]β-CIT in serial evaluation of human neuropsychiatric disease.

Key Words: iodine-123-β-CIT; SPECT; dopamine transporter

J Nucl Med 1996; 37:222–228

Iodine-123-β-CIT ([¹²³I]2β-carbomethoxy-3β-(4-iodophenyl-tropane) binds with high affinity to dopamine ($IC_{50} = 1.6$ nM) and serotonin ($IC_{50} = 3.78$ nM) transporters and has been used as a SPECT probe in human and nonhuman primates (1–5). In baboons, striatal activity was largely associated with dopamine transporters based on dynamic SPECT studies demonstrating displacement of this activity following administration of dopamine transporter-selective, but not serotonin transporter-selective agents (3). Following bolus administration of [¹²³I]β-CIT in humans, decay-corrected striatal time-activity data showed a prolonged time to highest uptake occurring by 18 hr posttracer injection and very slow striatal washout. Occipital and free parent plasma time-activity data achieved a plateau earlier than striatum and also demonstrated extremely slow rates of washout.

The ratio of striatal activity specifically bound to receptors divided by nondisplaceable activity is equal to the binding potential (BP) divided by the nonspecifically-bound compartment distribution volume (V_2) under conditions of equilibrium binding; i.e., when the concentration of parent compound is unchanging in plasma, receptor-bound, and nonspecifically-bound brain compartments. For a tracer like [¹²³I]β-CIT, the protracted steady levels of parent activity in plasma and activity within brain compartments closely approximates the equilibrium condition (5). Thus, the simple ratio of specific striatal to nondisplaceable activity calculated during the plateau phase of uptake provides an outcome measure that may be directly proportional to dopamine transporter density. Another consequence of the unchanging striatal time-activity data is the stability of other SPECT outcome measures, including specific striatal uptake expressed as a percent of injected radiopharmaceutical dose which provides a measure related to total receptor number.

The demonstration of reproducible SPECT outcome measures is critical and preliminary to the extension of [¹²³I]β-CIT to clinical populations, including the serial monitoring of progressive disorders like idiopathic Parkinson's disease. To extend our previous evaluation of quantitative [¹²³I]β-CIT SPECT outcome measures in humans, we undertook an evaluation of the test/retest reproducibility of two outcome measures